International Journal of Heat and Technology
Vol. 41, No. 5, October, 2023, pp. 1341-1348
Journal homepage: http://iieta.org/journals/ijht

Thermodynamic Modelling for the Prediction and Optimisation of Long-Term Performance in Wooden Structures

Chunyan Liu, Liyan Bai*

Architecture Department of Inner Mongolia University of Technology, Hohhot 010051, China

Corresponding Author Email: bailiyan@imut.edu.cn

https://doi.org/10.18280/ijht.410525

Received: 19 May 2023
Revised: 22 August 2023
Accepted: 29 August 2023
Available online: 31 October 2023

Keywords:
ancient architecture, wooden structures, thermodynamic model, Strain, chicken swarm optimisation algorithm, performance optimisation

ABSTRACT

Over time, ancient wooden structures undergo challenges in structural integrity and stability, influenced by various environmental conditions such as temperature fluctuations and humidity variations. Maintenance and protection of this invaluable architectural heritage require precise performance predictions and optimisations. While existing research has delved deeply into performance prediction of wooden structures, it predominantly focuses on empirical observations and experimental analyses, with minimal establishment and validation of theoretical models. Moreover, extant methods for prediction and optimisation often overlook the strain variation of wood under different temperatures and the stochastic nature of environmental factors. This study seeks to address this research gap by investigating the relationship between strain in the grain direction of ancient wooden beams and temperature, and by formulating a comprehensive thermodynamic model. Additionally, a novel optimisation approach using the chicken swarm optimisation (CSO) algorithm has been introduced to further refine performance parameters of wooden structures. By integrating the theoretical model with the CSO, this research offers a novel perspective and methodology for the prediction and optimisation of the long-term performance of wooden structures.

1. INTRODUCTION

Wooden structures, especially those found within ancient buildings, have long been regarded as invaluable architectural heritage due to their natural material attributes and historical traces [1-4]. Influenced by a myriad of environmental conditions, such as temperature fluctuations and changes in humidity over extended historical periods, these structures' physical properties are affected, and challenges are posed to their long-term structural integrity and stability [5-7]. Precise performance predictions and optimisations have emerged as pressing needs for the maintenance and protection of these architectural legacies.

Ancient wooden structures hold an irreplaceable position in history and culture [8-11]. Insights into their performance shifts under varying environmental conditions not only facilitate scientifically-grounded protective measures, ensuring prolonged safety and stability but also offer valuable references for modern wooden structure design and construction [12-17]. Moreover, by forecasting the long-term performance of wooden structures, scientific foundations can be provided for the restoration, reinforcement, and maintenance of ancient buildings, thus potentially extending their lifespan and preserving more historical heritage for future generations.

While numerous studies address the performance prediction of wooden structures, the majority place emphasis on empirical observations and experimental analyses, with fewer venturing into the establishment and validation of theoretical models [18-21]. Additionally, prevalent prediction methods often overlook wood's strain variations at different temperatures, which might result in prediction discrepancies. Furthermore, traditional optimisation approaches are primarily rooted in deterministic models, disregarding the stochastic nature of environmental factors, possibly rendering optimisation outcomes less accurate and robust.

In this study, a deep dive is taken into the relationship between strains in the grain direction of ancient wooden beams and temperature, culminating in the development of a comprehensive thermodynamic model. This establishes a robust theoretical foundation for the accurate prediction of wooden structures' performance under various environmental conditions. To further refine the performance parameters of these wooden structures, the CSO, a novel and efficient optimisation approach simulating the foraging behaviour of chicken flocks to locate optimal solutions, is introduced. By marrying these two core components, a novel and scientific methodology for the long-term performance prediction and optimisation of wooden structures is presented, bearing significant implications for both the protection of ancient architecture and applications in modern wooden constructions.

2. CONSTRUCTION OF THE THERMODYNAMIC MODEL FOR WOODEN STRUCTURES

Wooden beams in ancient buildings hold significant structural and cultural importance. Not only are they integral to the structural framework, but they also bear rich historical and cultural significance. Ensuring their long-term stability and safety becomes paramount. Over prolonged usage, such beams often undergo the influence of various environmental factors, with temperature fluctuations being one of the primary contributors. Thermal expansion and contraction, arising from temperature changes, can induce strains, adversely affecting the integrity and stability of these wooden structures.

While numerous studies have addressed the performance of wooden structures in ancient buildings, most are anchored in empirical observation and experimental analysis. By establishing a thermodynamic model, a more comprehensive and scientific perspective can be pursued, facilitating quantitative analysis and prediction of strain in these beams, thereby enhancing the scientific rigor and innovation of such studies. Given this backdrop, ancient wooden beams were selected as the study's subject. By adopting a thermodynamic approach, relationships between grain direction strain and temperature were investigated, laying the foundation for a more accurate theoretical guidance for the restoration, reinforcement, and maintenance of ancient buildings. Figures 1 and 2 respectively illustrate the free deformation and tenon-constrained deformation of ancient wooden beams.

Figure 1. Schematic of free deformation in ancient wooden beams

Figure 2. Schematic of tenon-constrained deformation in ancient wooden beams

For ancient wooden structures, especially for the study of mid-span beams, strain consideration is crucial, as it directly impacts the structural integrity and lifespan of the beams. Such beams, during their usage, are subject to the effects of various internal and external factors. Acknowledging this complexity, strain in the bottom grain direction of mid-span beams was bifurcated into two categories: strain induced by temperature changes and additional strain caused by the secondary bending effect exerted on the beam bottom by its ends.

Being a natural material, wooden exhibits a certain level of hygroscopicity and permeability, making it highly sensitive to temperature fluctuations. When temperature shifts, wooden undergoes thermal expansion or contraction, leading to strain within the structure. As temperature increases, activity between wood molecules intensifies, causing the wooden volume to expand and produce positive strain. Conversely, as temperature drops, reduced molecular activity results in volume contraction and negative strain. This type of strain is purely attributed to temperature variations and is independent of other factors.

Ancient wooden beams often bear substantial loads, such as roofing, decorations, and auxiliary facilities. These loads induce bending moments on the beams, causing them to bend. The constraint at the beam ends produces secondary bending moments at the beam's base, triggering additional strain. Thus, when these beams bear loads, compression is experienced at the top, while the bottom undergoes tension. However, due to constraints at the beam ends, the bottom cannot freely stretch, producing a bending moment that gradually intensifies from the ends towards the centre, known as the secondary bending moment. This moment elevates the strain at the beam's base, and the resultant increase in strain is termed as the additional strain.

Thermal mechanical modelling of the two forms of strain in ancient wooden beams is further explored in this section.

Parameters related to the strain, denoted as $\Delta\gamma_1$, due to thermal expansion and contraction in response to temperature changes incorporate aspects, such as longitudinal elasticity of the wood, longitudinal thermal expansion coefficient, temperature increment, stiffness, and length of the beam. These are specifically represented by R, β, ΔY, J_a and m respectively. When exposed to temperature fluctuations, the wooden beam undergoes either thermal expansion or contraction. The extent of change in the beam's length is determined by the longitudinal thermal expansion coefficient of the wood and the magnitude of temperature increment. In essence, a rise in temperature would make the beam attempt to expand, whereas a decrease would lead it to contract. However, such intuitive thermal expansions or contractions are not always free to occur. Particularly in ancient wooden beam structures, due to end constraints and the limitations imposed by other structural components, the beam cannot always expand or contract unreservedly. Consequently, when the beam attempts to expand or contract due to temperature variations, stresses are generated at its ends to counteract this deformation. Assuming the deformation of an ancient structural wooden beam during free expansion is represented by σ_Y, the actual deformation at the beam end is denoted as σ_I, and the deformation restrained by the beam end is σ_E. The counteractive force provided by the tension-compression spring at the beam end is represented by O. The following expressions describe the equilibrium of deformation at the beam ends:

$$\sigma_Y - \sigma_E = \sigma_I \tag{1}$$

$$\beta\Delta Ym - \frac{Om}{RS} = \frac{O}{J_a} \tag{2}$$

Considering that both ends of the beam are usually fixed, these ends produce reactive forces that resist strains induced by temperature variations. The magnitude of this reactive force depends on the length of the beam, its stiffness, and the longitudinal elasticity of the wood. Stiffness of the beam describes its resistance to deformation when subjected to external influences, such as loads or temperature fluctuations. Longitudinal elasticity of the wood, on the other hand, quantifies the extent of deformation the wood undergoes when subjected to external stresses. Assuming the end reactive force is represented by O and strain by $\Delta\gamma_1$, the following equations detail the respective calculations:

$$O = \frac{\beta\Delta YmR}{\frac{m}{S} + \frac{R}{J_a}} \tag{3}$$

$$\Delta\gamma_1 = \frac{O}{J_a m} = \frac{\alpha\Delta Y}{\frac{mJ_a}{SR} + 1} \tag{4}$$

Wooden beam connections in ancient structures are typically characterized as semi-rigid, rather than being fully rigid or simply hinged. This semi-rigidity introduces second-order bending moments to the beams, which in turn affect the overall structural stability and bending strain. The derivation for the additional strain $\Delta\gamma_2$, caused by the second-order bending effect from the beam end to its bottom, is outlined below.

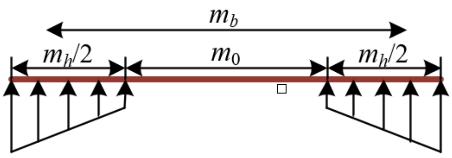

Figure 3. Principle of the calculated span of the ancient wooden beam

The calculated span of the beam is determined not solely by its actual length but also influenced by the stiffness of the end connections. The semi-rigid connection means that the actual calculated span of the beam might exceed its physical length, given that the flexibility of the connection increases the effective length of the beam. Figure 3 illustrates the principle behind the calculated span of ancient wooden beams. Assuming the arc wooden length is represented by m_h and the clear span of the beam by m_0, the following expression gives the calculation for the span of the beam:

$$m_b = m_0 + \frac{3}{4} m_h \tag{5}$$

In the context of semi-rigid connections, the bending moment at the beam end isn't a fixed value but varies. This varying moment is contingent on the stiffness of the connection and the magnitude of the applied load. Assuming that the fixed-end moments of a rigidly connected beam of the same size under identical loads are represented by L_{DS} and L_{DN}, the following expressions provide the calculation for the bending moment at the end of a beam with a semi-rigid connection:

$$L_S = \frac{L_{DS}(4\omega_S + 1) - 2L_{DN}\omega_N}{4\omega_N + 12\omega_S\omega_N + 4\omega_S + 1} \tag{6}$$

$$L_N = \frac{L_{DN}(4\omega_S + 1) - 2L_{DS}\omega_S}{4\omega_N + 12\omega_S\omega_N + 4\omega_S + 1} \tag{7}$$

Given the partial rigidity at the ends of the beam, the maximum bending moment at the base of the beam is also affected. This change in bending moment is influenced not only by the stiffness of the connection at the beam's end but also by the load distribution and the geometry of the beam. Let the rotational stiffness at both ends of the beam be represented by J_{eS} and J_{eN}. The expressions for ω_S and ω_N are given as:

$$\omega_S = \frac{RU}{J_{eS} m_b} \qquad \omega_N = \frac{RU}{J_{eN} m_b} \tag{8}$$

To consider the impact of semi-rigid connections on the stability of wooden beams, the introduction of computation length coefficients and moment amplification factors becomes necessary. These coefficients help in providing a more accurate description of how semi-rigid connections influence the overall stability of wooden beams. Let the amplification factor of the moment be represented by S_l. The equation below provides the formula for calculating the maximum bending moment at the beam's base after the end reaction provides the second-order bending:

$$L_{MAX} = L_0 + Ot_{MAX} = L_0\left(\frac{1}{1 - O/O_{ve}}\right) = L_0 S_l \tag{9}$$

Assuming the calculation length coefficient for the semi-rigid axial compression component is represented by ω, the critical load O_{ve} for the beam can be calculated using the formula:

$$O_{ve} = \frac{\tau^2 RU}{(\omega m)^2} \tag{10}$$

Considering the geometric imperfections of the beam and the effects of semi-rigid connections, the actual bending moment at the mid-span of the beam will usually exceed the bending moment based on linear-elastic analysis. This is referred to as the second-order bending moment, leading to an increase in the actual strain and deformation of the beam. Based on ω, the moment amplification factor S_l can be derived. The equation below represents the second-order bending moment at the mid-span of a wooden structure under rising temperature conditions:

$$\Delta L = (S_l - 1)L_0 \tag{11}$$

With all the aforementioned parameters and considerations, the additional strain caused by the second-order bending effect can be estimated. This additional strain is combined with the beam's original strain to determine the overall strain. Assuming the cross-sectional height of the beam is denoted by g, the formula below provides the calculation for the additional strain caused by the second-order bending:

$$\Delta\gamma_2 = \frac{\Delta L g}{2RU} = \frac{L_0 O g}{2RU(O_{ve} - O)} \tag{12}$$

The formula below provides the calculation for the strain in the grain direction at the mid-span of a wooden structure when the temperature increment is ΔY:

$$\Delta\varepsilon = \Delta\varepsilon_1 + \Delta\varepsilon_2 = \frac{O}{J_a m} + \frac{L_0 O g}{2RU(O_{ve} - O)} \tag{13}$$

For ancient wooden structures, cyclic temperature effects can lead to thermal expansion and contraction, resulting in strain. This cyclic process can be divided into four key stages. First, initial rise phase. From the starting state, the temperature begins to rise, causing the wooden structure to experience thermal expansion. Due to this temperature increase, thermal expansion commences, causing the strain in the grain direction to rise from its initial value. In this phase, strain is positively correlated with the temperature increment. Second, high-temperature stability phase. The temperature reaches its peak and remains relatively stable for a period. Consequently, the strain in the wooden structure also reaches its maximum. During this phase, since the temperature remains mostly constant, the strain in the wooden structure is relatively stable. Third, cooling phase. The temperature begins to drop from its peak, returning to a state similar to the starting conditions. Owing to this decrease, the wooden structure starts to contract, leading to a reduction in strain from its maximum value. During this phase, the strain is negatively correlated with the decrease in temperature. Finally, low-temperature stability phase. The temperature returns to its initial state and remains relatively stable during this phase. The strain in the wooden structure also returns to its initial state. With the temperature maintaining a low, stable condition, the strain within the wooden structure remains relatively consistent.

3. OPTIMISATION OF WOODEN STRUCTURE PERFORMANCE PARAMETERS

The influence of temperature on wooden structures cannot be overlooked. Such influence prompts expansion or contraction in the wood, thereby altering its internal stress and strain distribution. Through thermodynamic analysis, a deeper understanding of the specific impact of temperature variations on the performance of wooden structures has been achieved, providing a theoretical foundation for subsequent performance parameter optimisation. Not only can optimisation of these performance parameters enhance the stability of wooden structures, but it can also ensure their long-term safe use. Given the precious nature of ancient wooden architectural structures, this is of particular significance.

The design of the CSO aims to find the global optimal solution rather than getting trapped in local optima. This characteristic is essential in the complex problem of wooden structure performance parameter optimisation. The goal is to identify the best combination of parameters to ensure the performance and stability of the wooden structure. The CSO, endowed with significant adaptability, can handle a variety of performance parameters, adapting to different wooden structure characteristics and requirements. Detailed elaboration on the design steps of the algorithm follows.

Initial positions for several roosters are chosen randomly, representing different combinations of wooden structure performance parameters. Based on the performance model of the wooden structure, a fitness value is assigned to each rooster. This value indicates the superiority of that parameter combination. The position of the rooster with the highest fitness value is used as a reference to update the positions of other roosters, guiding the search direction towards a more optimal area. Let the position of the u-th individual during the y-th iteration be denoted by $z_{u,k}(y)$. A Gaussian distribution function with a mean of 0 and a standard deviation of δ^2 is given by $rand(0,\delta)$. The fitness value of the individual u is represented by d_u, while a sufficiently small positive number is denoted by γ. Excluding the u-th individual, the identifier of any rooster individual is given by j. The update mechanism for the position of the rooster is expressed as follows:

$$z_{u,k}(y+1) = z_{u,k}(y) * \left(1 + rand\left(0, \delta^2\right)\right) \tag{14}$$

$$\delta^2 = \begin{cases} 1, d_u < d_j \\ \exp\left(\dfrac{d_j - d_u}{|d_u| + \gamma}\right), d_u > d_j \in [1, B_j], j \neq u \end{cases} \tag{15}$$

Similarly, the position of the hen is chosen at random. Using the same approach as the rooster, a fitness value is allocated to each hen. Hens primarily conduct local searches, selecting a relatively small neighbourhood range to explore areas near the current optimal position in search of superior solutions. If the identifier of the rooster in the sub-group where the u-th hen is located is $e1$, and the identifier of a randomly selected rooster or hen is $e2$ (with $e1 \neq e2$), and a random number within the range [0,1] is represented by *rand*, then the position update mechanism for the hen is provided by:

$$\begin{aligned} z_{u,k}(y+1) &= z_{u,k}(y) + A_1 * rand \\ &* \left(z_{e1,k}(y) - z_{u,k}(y)\right) \\ &+ A_2 * rand * \left(z_{e2,k}(y) - z_{u,k}(y)\right) \end{aligned} \tag{16}$$

$$A_1 = \exp\left(\frac{d_u - d_{e1}}{|d_u| + \gamma}\right) \tag{17}$$

$$A_2 = \exp\left(d_{e2} - d_u\right) \tag{18}$$

The positions of chicks are determined based on the locations of their corresponding hens; they conduct searches around their hens. If a chick identifies a solution superior to that of its hen, the hen updates its position, thereby adopting the chick's solution, which facilitates the inheritance of fitness. Let the position of the mother hen of the u-th chick during the y-th iteration be denoted by $z_{l,k}(y)$, and the following coefficient by *DM*. The update mechanism for the chick's position is expressed as:

$$z_{u,k}(y+1) = z_{u,k}(y) + DM * \left(z_{l,k}(y) - z_{u,j}k(y)\right) \tag{19}$$

The core objective elucidated in this study revolves around the application of the CSO to optimise the performance parameters of wooden structures, drawing insights from thermal analysis and prediction outcomes of ancient wooden architecture. This constitutes a multistage, structured process. Initially, a thermodynamic analysis of ancient wooden architecture was performed to grasp the reactions and alterations of wood under diverse temperature conditions. This involved studying the expansion and contraction behaviours of wood at varying temperatures and the consequent implications for the overall stability of wooden structures. Following this analysis, an optimisation problem concerning wooden structure performance parameters was formulated. Though potentially high-dimensional, involving numerous performance parameters, this problem was transformed into a bidimensional minimisation task, thereby effectively curtailing computational complexity and bolstering optimisation efficiency. The CSO was selected as the preferred optimisation tool, given its aptitude for global optimum search, especially well-suited for intricate optimisation problems. Employing the CSO, the solution space was systematically navigated. In each iteration, relying on the position update rules for roosters, hens, and chicks, the solution was continuously adjusted to approximate the optimum. Once optimal parameters for timber structure performance are identified, they are applied to actual models of ancient wooden structures to validate their real-world efficacy.

For the optimisation of wooden structure performance parameters, pertinent design variables and optimisation objectives were determined. Physical property variables encompassed wood density, elastic modulus of the wood, tensile strength, compressive strength, and shear strength of the wood. Structural dimension variables included maximum and minimum sizes of beams, columns, and other structural elements, as well as designs of nodes or joints. Finally, technological variables covered wood dryness and manufacturing techniques. These variables are direct influencers of wooden structure performance and are adjustable within certain bounds.

Subsequently, the objective function for wooden structure performance optimisation is established. This step is pivotal as it delineates the goals to be achieved during the optimisation process. Within the ambit of wooden structure performance enhancement, the objective function ought to encapsulate key performance indicators of the wooden structure, tailored based on actual requirements and project objectives.

In terms of stability, since a structure's stability under various loads and environmental conditions is a fundamental performance indicator, an objective function was defined with the aim to maximise the stability of the wooden structure under specified conditions, or to ensure stability remains above a particular safety threshold. For durability considerations, given wood's vulnerability to environmental factors such as humidity, temperature, and biological attacks, another objective function was designed aiming to maximise the expected lifespan of the wooden structure or to minimise the frequency and cost of maintenance and repairs. In terms of stiffness and strength, which are pivotal parameters dictating deformation and failure of wooden structures under load, an objective function was conceptualised with the intent to maximise structural stiffness and/or strength, ensuring the structure can endure anticipated loads without excessive deformation or damage. Recognising the limited and sustainable nature of wood resources, an objective function was introduced to minimise the amount or volume of required wood while meeting other performance benchmarks.

Thus, the objective function might be represented as:

$$\begin{aligned} f(x) &= \alpha_1 \times stability\ index(x) \\ &+ \alpha_2 \times durability\ index(x) \\ &+ \alpha_3 \times rigidity\ index(x) \\ &+ \alpha_4 \times material\ utilisation\ index(x) \end{aligned} \tag{20}$$

where, x denotes the design variables and α_i signifies the weights associated with each index, adjustable based on specific project requirements.

4. EXPERIMENTAL RESULTS AND ANALYSIS

An in-depth investigation was conducted into the relationship between strain along the grain direction of ancient wooden beams and temperature. A comprehensive thermodynamic model was established, providing a robust theoretical foundation for predicting the performance of wooden structures under various environmental conditions. Examination of the aforementioned Figure 4 reveals a specific pattern of strain variation over time in the grain direction of the ancient wooden beam. Between time intervals 0 and 8, the strain of the wooden beam remained relatively stable, with only minor fluctuations. This stability is possibly attributed to negligible impacts from temperature and other external factors during this period. A pronounced increase in strain is observed between time units 8 and 9, indicating a significant change. This sudden increase might have been caused by sudden external influences such as a sharp rise in temperature, a sudden change in humidity, or an increased external load. Following this abrupt increase, the strain gradually stabilised and maintained a consistent growth trend in the subsequent timeframe. It is indicated that at this stage, although external conditions continue to change, the impact on the wooden beam remains relatively stable, with no apparent abrupt changes observed. It can be inferred that the strain in ancient wooden beams is closely related to temperature and other environmental factors. For the majority of the time, the strain remains relatively stable under consistent external conditions. However, abrupt environmental changes, such as sharp temperature rises or humidity shifts, can cause sudden strain variations, potentially posing risks to the wooden structure. Monitoring and preventative measures are essential.

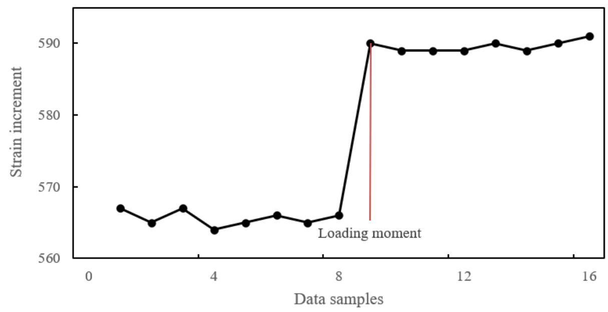

Figure 4. Strain increment diagram of unconstrained ancient wooden beam during loading

The strain increments in ancient wooden beams, as depicted in the previous Figure 5, were analysed. Between 20:00 and 8:00, regardless of whether under "unconstrained" or "constrained" conditions, a declining trend in strain increment was observed. The decline was more pronounced under "constrained" conditions. By 8:00, the strain increments under both conditions approached their lowest points. From 8:00 to 20:00, under "unconstrained" conditions, the strain increment began to rise gradually in the morning until around 16:00, after which a slight decrease was observed. Conversely, under "constrained" conditions, a more evident growth trend was observed from the morning until about 16:00, after which a decline commenced. By 20:00, the strain increment under "constrained" conditions remained higher than that under "unconstrained" conditions. Throughout the observation period, the variation in strain increment under "constrained" conditions was greater than that under "unconstrained" conditions. This greater variation might be attributed to the increased external influences imposed by the constraints. It is evident that the strain increment in ancient wooden beams correlates with time and external environmental factors such as temperature. Regular monitoring of these beams, taking into account actual constraint conditions, is essential to ensure their safety and stability.

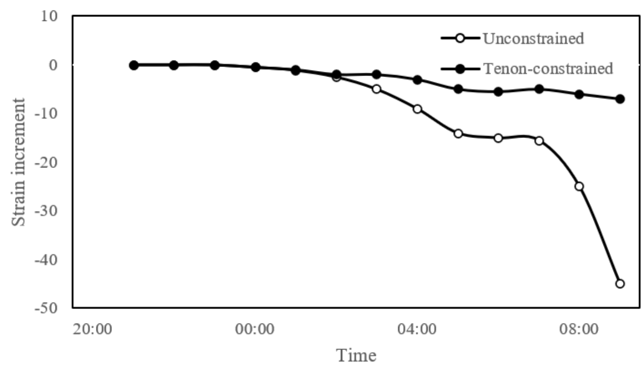

1) Night

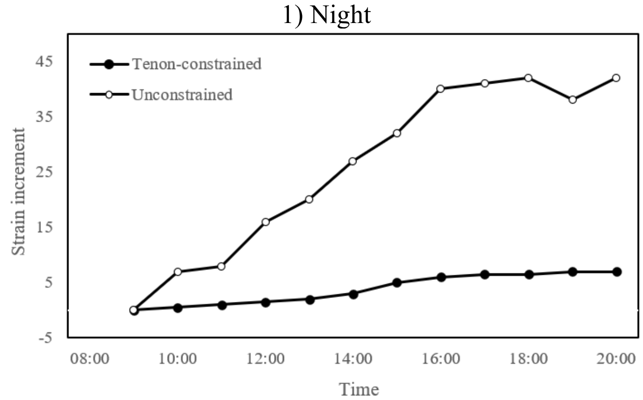

2) Day

Figure 5. Comparative analysis of strain increment in ancient wooden beams under different constraint conditions

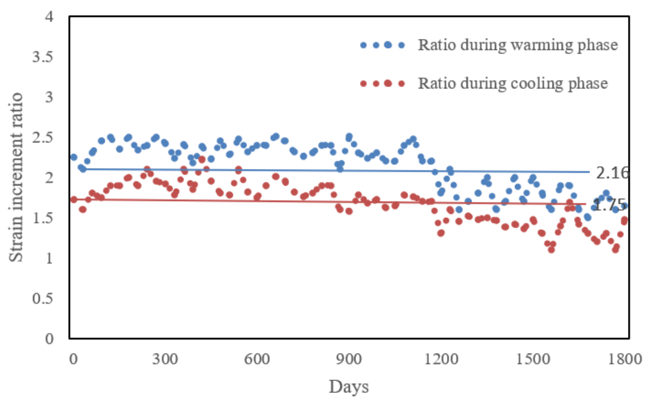

Figure 6. Long-term strain increment ratio of ancient wooden beams under different temperature environments

As shown in Figure 6, Based on the depicted long-term strain increment ratios in ancient wooden beams and the prior discussion, further analysis was conducted. Both datasets showed a dispersed trend with increasing temperature, yet most data points congregated around their respective average lines. Data points for the warming phase primarily clustered around an average value of 2.16. Despite a few outliers, the majority of the data points fall within the 2.0 to 2.3 range, suggesting minimal variation in the strain increment ratio during warming. For the cooling phase, data points predominantly clustered around an average of 1.75, notably lower than the warming phase's average. Most of these data points fall within the 1.7 to 2.0 range.

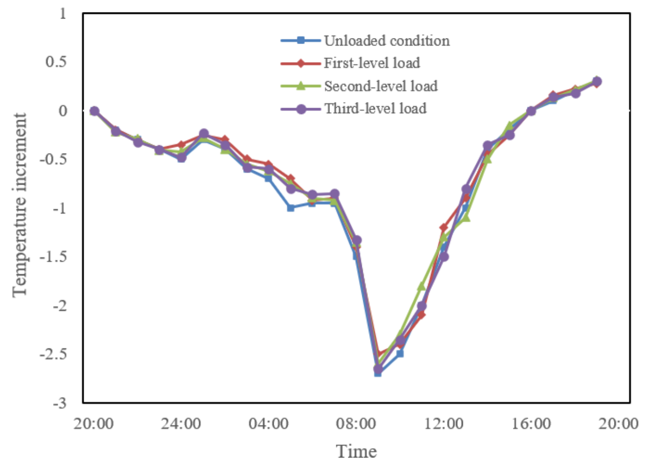

1) Temperature increment

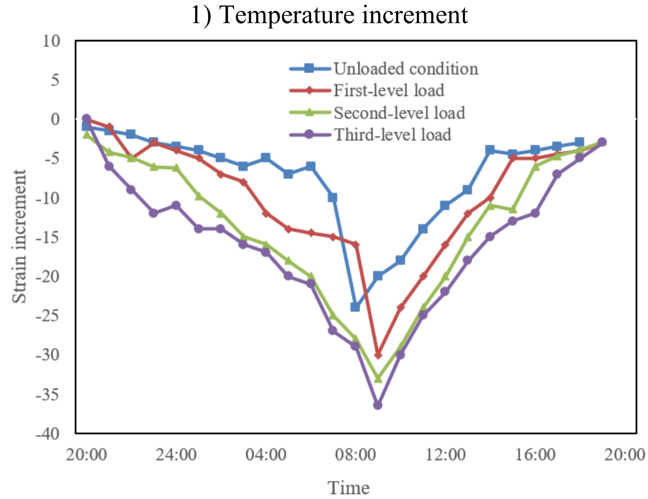

2) Strain increment

Figure 7. Comparison of temperature and strain increments under various loads with tenon constraints in ancient wooden beams

Analysing Figure 7, several conclusions can be drawn concerning the temperature and strain increments in ancient wooden beams under various load conditions with tenon constraints. In all observed scenarios, the temperature increment displayed a similar pattern: initially declining with time, reaching a nadir at dawn, and subsequently ascending. This pattern persisted regardless of the applied load, although slight differences were observed between individual loading conditions. As for the strain increment, it paralleled the trend of temperature increment, first declining to its lowest point, then gradually rising. Wooden beams without tenon constraints demonstrated relatively minor fluctuations in strain increment, whereas those with tenon constraints exhibited more significant variations. This might be attributed to the constraints restricting the freedom of movement in the beams, rendering them more susceptible to temperature variations. Under differing load conditions, the strain increment pattern remained roughly analogous, though the magnitude of fluctuations differed. Thus, a correlation can be discerned between temperature and strain increments in ancient wooden beams under various loads with tenon constraints. The constraints on the tenon heightened the beam's sensitivity to temperature variations, with the magnitude of the applied load further influencing this sensitivity. The strain increment in the wooden beams also changed in response to temperature variations, a trend more pronounced when tenon constraints were applied.

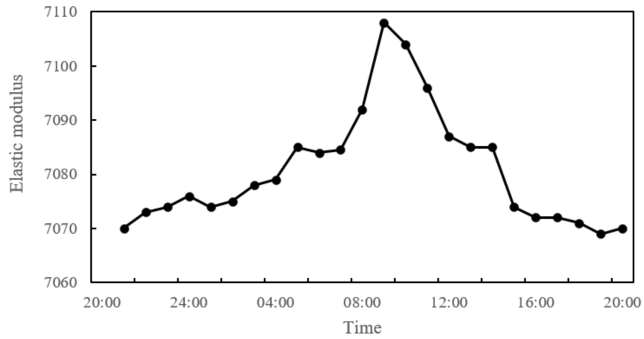

1) Elastic modulus

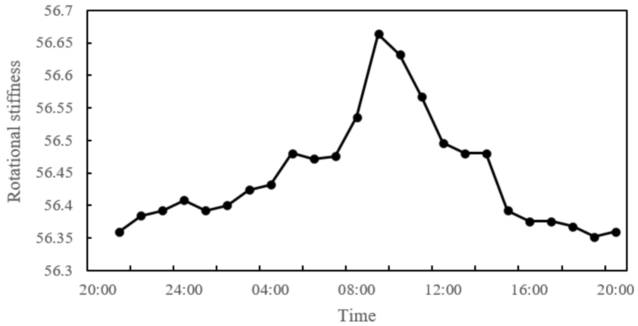

2) Rotational stiffness

Figure 8. Elastic modulus and rotational stiffness during loading under tenon constraints in ancient wooden beams

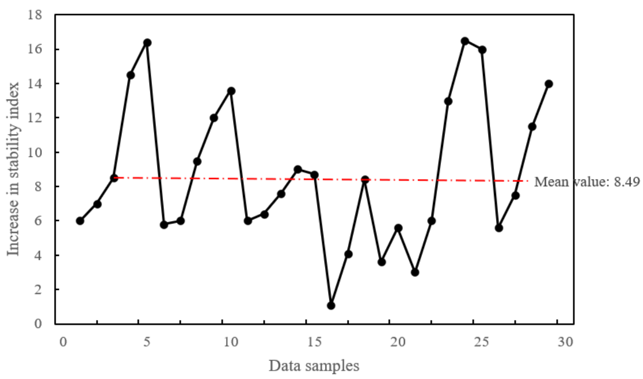

1) Stability index

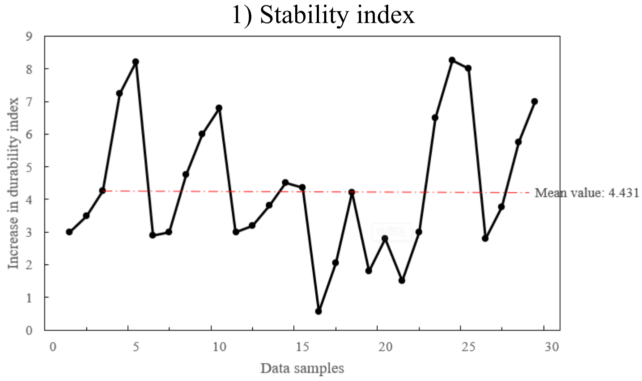

2) Durability index

Figure 9. Rise in stability and durability indices in ancient wooden beams under various conditions

Observations from Figure 8 indicate trends in the elastic modulus and rotational stiffness in ancient wooden beams under tenon constraints. Both the elastic modulus and rotational stiffness displayed analogous tendencies: from 20:00 in the evening until 16:00 the next day, both metrics surged before swiftly descending. The peak values for both the elastic modulus and rotational stiffness were reached around noon, suggesting external factors during this period, such as temperature and humidity, might exert the most substantial impact on the beam's properties. It can be concluded that, under tenon constraints, both the elastic modulus and rotational stiffness of the ancient wooden beams were influenced by external environmental factors, particularly during the midday hours. While both demonstrated similar trends, the absolute change in the elastic modulus exceeded that of the rotational stiffness. For the maintenance and preservation of ancient structures, the midday period merits special attention as the beam's performance might be most significantly affected at this time.

Based on Figure 9, a comparative analysis of the rise in stability and durability indices in ancient wooden beams under diverse conditions can be undertaken. In the graph depicting "rise in stability", the stability index exhibited fluctuations; in certain conditions, there was a marked enhancement in stability, while in others, a slight decline was evident. An average stability value of 8.49 was established, serving as a benchmark for evaluating stability across various conditions. In the "rise in durability" graph, durability too displayed a fluctuating trend with an average durability index of 4.431. It can be inferred that, within the considered conditions, both the stability and durability indices of ancient wooden beams experienced an upward shift, indicative of optimised performance parameters.

5. CONCLUSION

In-depth research was conducted into the relationship between strain in the longitudinal direction of ancient wooden beams and temperature, leading to the construction of a comprehensive theoretical thermodynamics model. Additionally, to further optimise the performance parameters of wooden structures, the CSO, mimicking the foraging behaviour of flocks of chickens to identify optimal solutions, was incorporated. From the analyses presented, pronounced strain variances in ancient wooden beams under varying temperature conditions were evident. A certain correlation between these strain disparities and temperature variations offers potential for predicting performance changes in wooden structures under various environmental conditions. In the longitudinal direction, the relationship between strain and temperature was rigorously investigated, culminating in the development of a theoretical thermodynamics model that provides significant theoretical backing for subsequent experiments. The integration of the CSO to identify the optimal solution, by emulating chicken foraging behaviour, offers a novel method for enhancing the performance parameters of wooden structures. The provided figures indicate improvements in stability and durability indices of ancient wooden beams under diverse operational conditions, further attesting to the efficacy of the CSO in wooden structure performance optimisation.

In summary, the strain properties of ancient wooden beams under varying temperatures were successfully investigated, and a corresponding theoretical model was established. Moreover, with the incorporation of the CSO, effective optimisation of wooden structure performance parameters was achieved. These findings offer pivotal insights for the preservation and restoration of ancient wooden architectural structures and carry significant implications for the design and application of modern wooden structures.

REFERENCES

[1] Wang, Z., Yang, N. (2022). Evaluation of bending strength of ancient building wood by multi-point nondestructive testing method. Journal of Hunan University Natural Sciences, 49(1): 78-84. https://doi.org/10.16339/j.cnki.hdxbzkb.2022009

[2] Yang, Y., Li, B., Liu, Y., Zhang, W., Wang, C. (2023). Identification of tree species and extent of material deterioration of wood components in the yangjia courtyard ancient building. Forest Products Journal, 73(2): 82-93. https://doi.org/10.13073/FPJ-D-22-00068

[3] Liu, B., Fu, Y.J., Ma, X., Lu, Y., Wang, L. (2021). Relationship between wood species selection and biological diseases of ancient building wooden components in severe wood biological diseases area. Scientia Silvae Sinicae, 57(12): 108-121. https://doi.org/10.11707/j.1001-7488.20211211

[4] Chen, L.K., Li, S.C., King, W.S., Jiang, L.Z., Luo, H.Z., Li, Q.J. (2020). How the decayed straight mortise-tenon joints influence the seismic performance of ancient timber building? Evidence from experiment scenarios of the benchmark wood frames. Engineering Failure Analysis, 116: 104685. https://doi.org/10.1016/j.engfailanal.2020.104685

[5] Ma, X., Li, J., Wang, L., Wang, Y. (2022). Damage of coleoptera longhorned beetles in wooden components of ancient buildings in China. Scientia Silvae Sinicae, 58(12): 130-140. https://doi.org/10.11707/j.1001-7488.20221212

[6] Zhang, B., Ma, X., Jiang, M., Li, X. (2021). Preparation and effect evaluation of organic preservative for ancient buildings wood biodeterioration. Scientia Silvae Sinicae, 57(8): 167-175. https://doi.org/10.11707/j.1001-7488.20210817

[7] Zhang, B., Shi, L., Fan, J. (2021). Discussion on the value of nanomaterial strength during the renovation and strengthening of ancient wooden structures. Integrated Ferroelectrics, 216(1): 214-230. https://doi.org/10.1080/10584587.2021.1911270

[8] Yang, N., Wang, Z. (2022). Influence of number and position of measuring points on the nondestructive testing method to predict the flexural modulus of aged wood. Holzforschung, 76(5): 421-429. https://doi.org/10.1515/hf-2021-0065

[9] Wang, Y., Wang, W., Zhou, H., Qi, F. (2022). Burning characteristics of ancient wood from traditional buildings in Shanxi Province, China. Forests, 13(2): 190. https://doi.org/10.3390/f13020190

[10] Ma, X., Wang, L., Qiao, Y., Duan, E., Lu, Y., Fang, X., Zhang, B., Wang, Y., Jin, Q. (2022). Evaluation of damage grades for wooden components of ancient buildings based on nesting habits of carpenter bee. Scientia Silvae Sinicae, 58(3): 167-174.

[11] Deng, J., Liu, T.S., Yao, M., Yi, X., Bai, G.X., Huang, Q.R., Li, Z. (2023). Comparative study of the combustion and kinetic characteristics of fresh and naturally aged pine wood. Fuel, 343: 127962. https://doi.org/10.1016/j.fuel.2023.127962

[12] Chang, L.H., Chang, X.H., Chang, H., Qian, W., Cheng, L.T. (2021). The predictive research of ancient wooden building internal defects compressive bearing capacity based on nondestructive testing methods. Mechanics of Advanced Materials and Structures, 28(3): 252-259. https://doi.org/10.1080/15376494.2018.1556826

[13] Yang, Y., Li, B., Sun, H., Fan, Y., Wang, A., Zhao, R., He, Y. (2022). Study on the decay extent of wooden components of Danxia Temple ancient building by polarized light, fluorescence and X-ray diffraction methods. Cellulose Chemistry and Technology, 56(7-8): 717-726.

[14] Zhang, L., Chen, Z., Dong, H., Fu, S., Ma, L., Yang, X. (2021). Wood plastic composites based wood wall's structure and thermal insulation performance. Journal of Bioresources and Bioproducts, 6(1): 65-74. https://doi.org/10.1016/j.jobab.2021.01.005

[15] Deng, H. (2022). Application of BIM technology in the seismic performance of “Wood Weaving” structure of wooden arcade bridges. Shock and Vibration, 2022: Article ID 8033059. https://doi.org/10.1155/2022/8033059

[16] Xue, J., Yuan, Z., Ren, G., Qi, L., Zhang, W., Wei, J. (2022). Seismic performance of glued-laminated wood frame and frame brace structure: Experimental and finite element analysis. Journal of Building Engineering, 48: 103944. https://doi.org/10.1016/j.jobe.2021.103944

[17] Brege, S., Nord, T., Brege, H., Holtström, J., Sjöström, R. (2022). The Swedish wood manufacturing sector: findings from a contextually adapted structure-conduct-performance model. Wood Material Science & Engineering, 17(6): 878-886. https://doi.org/10.1080/17480272.2021.1969594

[18] Wong, J. (2021). Case study of SFU parcel 21, a high-performance mid-rise wood frame residential structure. World Conference on Timber Engineering 2021, WCTE 2021.

[19] Akpan, E., Friedrich, K., Jacob, S., Thines, E., Wetzel, B. (2021). Reactive layer assembly sustains an interlocked structure in green processed and scalable high-performance layered wood. ACS Sustainable Chemistry & Engineering, 9(47): 15744-15754. https://doi.org/10.1021/acssuschemeng.1c03468

[20] Fang, S., Liu, Y., Yue, J., Tian, Y., Xu, X. (2021). Assessments of growth performance, crown structure, stem form and wood property of introduced poplar clones: Results from a long-term field experiment at a lowland site. Forest Ecology and Management, 479: 118586. https://doi.org/10.1016/j.foreco.2020.118586

[21] Sun, Y., Zhang, Q., Clark, J.H., Graham, N.J., Hou, D., Ok, Y.S., Tsang, D.C. (2022). Tailoring wood waste biochar as a reusable microwave absorbent for pollutant removal: structure-property-performance relationship and iron-carbon interaction. Bioresource technology, 362: 127838. https://doi.org/10.1016/j.biortech.2022.127838